

Quantum dots in glass spherical microcavity

Rui Jia,^{a)} De-Sheng Jiang, Ping-Heng Tan, and Bao-Quan Sun

National Laboratory for Superlattices and Microstructures, Institute of Semiconductors, P. O. Box 912, Beijing 100083, People's Republic of China

(Received 8 January 2001; accepted for publication 1 May 2001)

Glass spherical microcavities containing $\text{CdSe}_x\text{S}_{1-x}$ semiconductor quantum dots (QDs) are fabricated. The coupling between the optical emission of embedded $\text{CdSe}_x\text{S}_{1-x}$ QDs and spherical cavity modes is realized. When the luminescence of QDs is excited by a laser beam, the strong whispering gallery mode resonance with high Q factors is achieved in the photoluminescence spectra. © 2001 American Institute of Physics. [DOI: 10.1063/1.1380732]

Recently, the fabrication and optical properties of different kinds of planar microcavities which contain semiconductor nanoclusters or quantum dots (QDs) have attracted much efforts,^{1–6} while the works about spherical or cylindrical microcavities embedded with semiconductor QDs are scarce. A spherical three-dimensional optical microcavity can be made of a nonabsorbing microsphere with a higher refractive index than the surrounding medium, having a diameter comparable to or slightly larger than the light wavelength, i.e., a few microns. In such microcavities, there exist a number of discrete resonant optical modes, the so-called whispering gallery modes (WGMs).^{7,8} It is well known that II–VI semiconductor compound QDs can be grown in different matrices by different manufacturing processes.^{9,10} When semiconductor QDs are embedded in the spherical microcavity, the QD luminescence can couple with the WGMs, and a lower threshold of stimulated emission (or lasing modes) of QDs may be realized. Artentev and Woggon prepared spherical microcavities using a chemical way.⁸ They embedded CdSe semiconductor QDs in the poly(methylmethacrylate) microsphere and realized the coupling of electronic and photonic states.

We have used an approach to prepare glass microspheres embedded with $\text{CdSe}_x\text{S}_{1-x}$ semiconductor QDs, which have a better optical stability than the polymer microspheres prepared by usual chemical approaches because the latter are often degraded under strong illumination due to the photosensitive surface reactions. The resonant WGMs are observed in the glass microspheres with QDs for the luminescence bands of both excitonic transitions and from surface defect states of the embedded QDs. The high Q values of quality factor are realized for WGMs.

For preparing optical microspheres containing semiconductor QDs, we have used commercially available glass ingots that are a source material for making optical filter glasses, for example, RG645 or other types in the same series. The glass has a refractive index of 1.5 or larger, being suitable to employ as the microcavity media surrounded by the air ($n=1$). The glass ingots contain CdO, CdS, and elemental sulfur or selenium⁹ in their composition. They were at first pulverized into small glass pieces, with the size of a few micrometers and sifted by sieves. Then, a specially designed gas burner was employed to heat and blow off

micrometer-sized glass pieces. In this heating process the glass pieces were melted at a temperature higher than the softening point and formed into microspheres due to the surface tension. The obtained microspheres were annealed at certain temperature for several hours in order to form precipitates and grow $\text{CdSe}_x\text{S}_{1-x}$ nanoclusters in the microspheres. The size of $\text{CdSe}_x\text{S}_{1-x}$ semiconductor nanocrystals depends on the annealing temperature and time.^{9,10}

Raman scattering and photoluminescence (PL) spectra of the glass microspheres embedded with $\text{CdSe}_x\text{S}_{1-x}$ QDs are measured in a backscattering geometry by using the Dilor Super Labram Microraman system, with a typical spectral resolution of 1 cm^{-1} . The spatial resolution of less than $2\text{ }\mu\text{m}$ is achieved using a microscope with a $100\times$ objective lens. The image of annealed microspheres can be examined under the lamp illumination, as shown in Fig. 1. The microsphere shown in the image has a perfect surface, with a diameter of $41\text{ }\mu\text{m}$.

The Raman spectra of unannealed and annealed microspheres were measured as shown in Fig. 2. The Raman signals from the microsphere sample annealed at $600\text{ }^\circ\text{C}$ for 10 h are strong for both CdSe-like longitudinal optical (LO) phonon and CdS-like LO phonon modes, located at 208.3 cm^{-1} and 280.3 cm^{-1} , respectively, in agreement with what expected by the two-mode behavior of the lattice vibrations in $\text{CdSe}_x\text{S}_{1-x}$ alloy.^{11,12} It confirms that the $\text{CdSe}_x\text{S}_{1-x}$ clusters are formed after the annealing process. It is found that the composition ratio of Se and S in $\text{CdSe}_x\text{S}_{1-x}$ alloy is nearly 80:20, which has no essential change with increasing annealing time, indicating that the $\text{CdSe}_x\text{S}_{1-x}$ QDs only grow in size but do not change their composition during the annealing process.

Figure 3(a) depicts the PL spectra from two microsphere samples annealed at $580\text{ }^\circ\text{C}$ and $600\text{ }^\circ\text{C}$ for 10 h, excited by an Ar^+ laser operating at 488.0 nm , respectively. There are two peaks existing in the room temperature PL spectra for the microsphere samples. The peak at higher energy side is sharp, while the peak at lower energy side is broader. We assign the sharp peak ($P1$) to the excitonic transitions of $\text{CdSe}_x\text{S}_{1-x}$ QDs. The broad peak ($P2$) with strong intensity is assigned to the surface defect states related luminescence. These defect states may be the nonstoichiometric defects on the cluster surfaces.⁹ When the heat treatment temperature increases from $580\text{ }^\circ\text{C}$ to $600\text{ }^\circ\text{C}$, the peak position of exci-

^{a)}Electronic mail: jiarui@red.semi.ac.cn

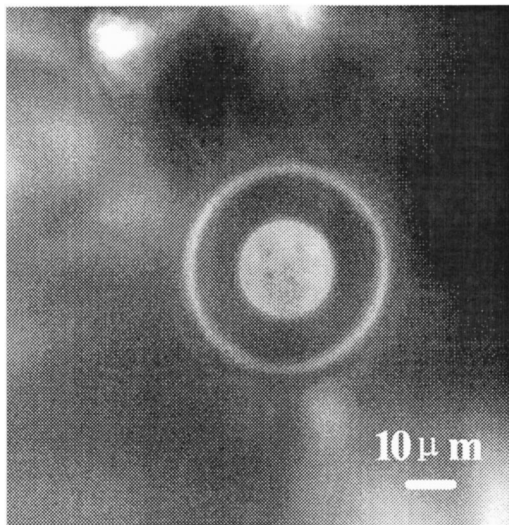


FIG. 1. Optical image of a prepared glass microsphere with the diameter of $41 \mu\text{m}$ is shown.

tonic transitions shifts from 2.17 eV to a lower energy of 2.05 eV . The redshift of the peak position is assigned to the increase in size of $\text{CdSe}_x\text{S}_{1-x}$ QDs due to the heat treatment at a higher temperature. It is noted that in order to form uniform nanoclusters and keep a perfect surface of annealed glass microspheres, the heat treatment temperature should be selected within a certain range below the softening temperature of the glass. We found that 580°C – 600°C is an appropriate temperature range for the annealing. In addition, the PL excitation (PLE) spectra were measured for microspheres by using a fluorescence spectrometer in order to characterize the absorption of the samples. The room temperature PLE spectrum (solid line) of the microsphere samples annealed at 600°C , detected at 1.55 eV , is shown in Fig. 3(b) together with the PL spectrum (dashed line) excited by a Xe lamp light operating at the wavelength of 450 nm . There are two peaks in the PLE spectrum which are assigned to the ground and the first excited excitonic transitions, $1S_{3/2}-1S_e$ and $2S_{3/2}-1S_e$, respectively.^{13,14} As the PLE spectra reflect the absorption properties of the samples, a Stokes shift of about 138 meV determined between the absorption peak $1S_{3/2}-1S_e$ and the luminescence peak $P1$ from the shift between the corresponding PLE and PL peaks.

It is found that the annealed microsphere samples exhibit

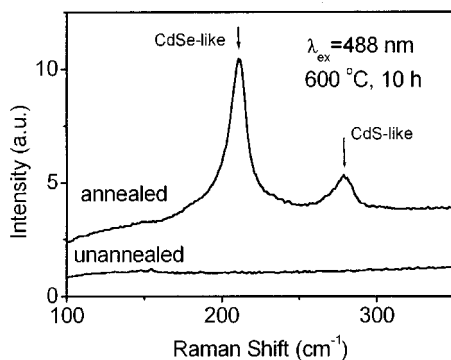


FIG. 2. Raman spectra of the single annealed and unannealed glass microspheres measured at room temperature and in a back scattering configuration are shown. The wavelength of excitation laser light is 488.0 nm .

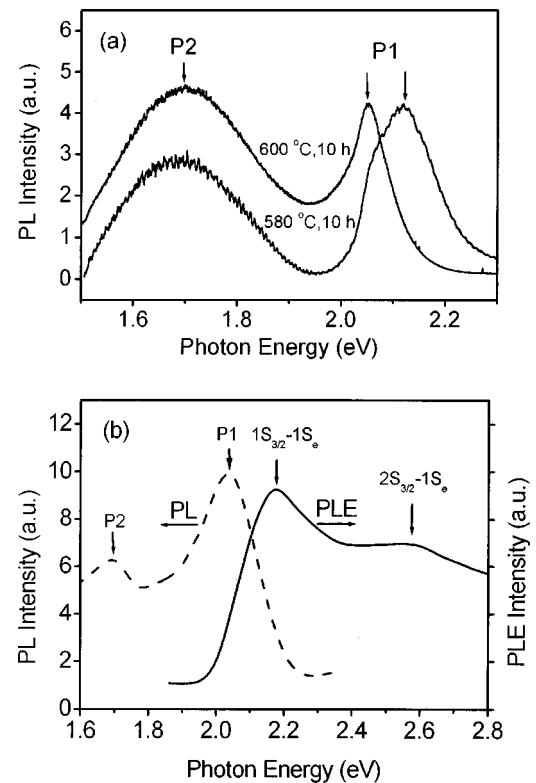


FIG. 3. (a) Room temperature PL spectra of two microspheres with $\text{CdSe}_x\text{S}_{1-x}$ QDs annealed at 580°C and 600°C , respectively, are shown. (b) The comparison between PL (dashed line) and PLE (solid line) spectra of the microsphere sample annealed at 600°C . The PL spectrum is excited by a Xe lamp at a wavelength of 450 nm . The detection photon energy of the PLE spectrum is 1.55 eV .

a structure of periodic sharp peaks superimposed on the two PL bands when the excitation light is focused on the microsphere near the inner surface. Figure 4(a) shows the emission spectra of an annealed single microsphere excited by 488.0 nm laser line. Many regularly spaced sharp peaks were observed to superimpose on the PL bands. These sharp peaks can be ascribed to the resonant microspherical cavity modes. In addition, the intensity of resonance peaks is different in different wavelength regions. The intensity of resonance peaks superimposed on the band at the lower energy side is stronger than those superimposed on the band of higher energy. Details of the WGMs peak structure are shown in Fig. 4(b) after subtracting the Gaussian background line shape of two PL bands of QDs. Based on the Mie Scattering theory,¹⁵ the separation between the adjacent peak wavelengths of the WGM resonance modes, $\Delta\lambda$, is approximately given by

$$\Delta\lambda = \frac{\lambda^2 \tan^{-1}\{(n_1/n_2) - 1\}^{1/2}}{\pi n_2 d \{(n_1/n_2) - 1\}^{1/2}}, \quad (1)$$

where λ and d ($\sim 41 \mu\text{m}$) are the emission wavelength and the diameter of the measured microsphere, respectively, n_1 and n_2 represent the refractive indices of the sphere ($n_1 \sim 1.523$) and the surrounding air ($n_2 \sim 1.0$), respectively. The calculated value for $\Delta\lambda$ at the intrinsic spectral range of 605 nm and at the surface defect luminescence range of 690 nm are 2.16 nm and 2.66 nm , respectively, which agrees well with the observed mode spacing, $\Delta\lambda_1$ and $\Delta\lambda_2$ of 2.12 and 2.74 nm , as shown in Fig. 4(b). The small peaks between the regular-spaced peaks are ascribed to the different resonance

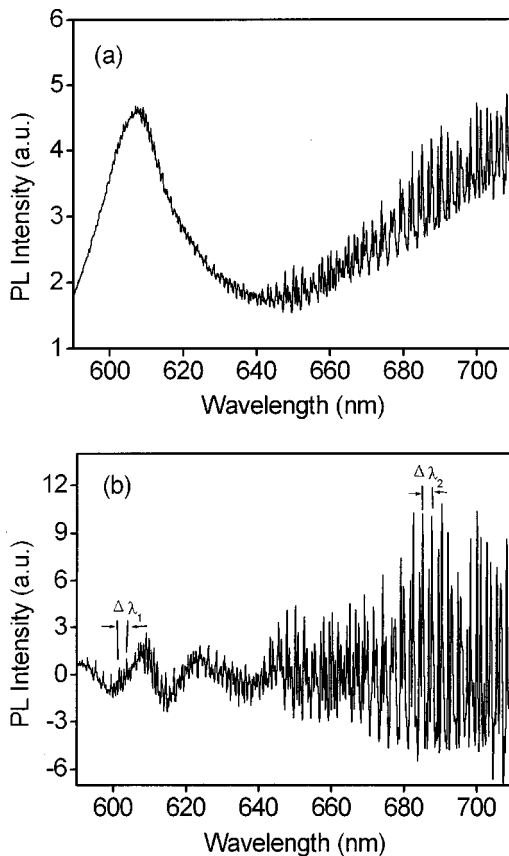


FIG. 4. (a) Room temperature PL spectrum of a single microsphere with $\text{CdSe}_x\text{S}_{1-x}$ QDs annealed at 600°C are shown. The excitation wavelength is 488.0 nm . (b) Normalized photoluminescence spectrum of (a) after subtracting the luminescence background of QDs, showing clearer WGM. The separations between the adjacent peak wavelengths of the resonant WGMs, $\Delta\lambda_1$ and $\Delta\lambda_2$, are shown by arrows.

mode and order numbers in the microsphere and will not be discussed here. We have also calculated the value of quality factor Q . The Q value can be given by¹⁵

$$Q = \frac{\hbar\omega_0}{2\hbar\gamma}, \quad (2)$$

where $2\hbar\gamma$ is the Lorentzian fitting to the linewidth of the cavity modes and $\hbar\omega_0$ is the photon energy. At the wavelength of $\lambda = 605\text{ nm}$ ($\hbar\omega = 2.05\text{ eV}$), the Lorentzian fit of the linewidth for the resonance mode is about $2\hbar\gamma = 0.0022\text{ eV}$. From formula (2), we can get the quality factor Q at the intrinsic PL band $P1$ is about 930. At the wavelength of $\lambda = 692\text{ nm}$ ($\hbar\omega = 1.79\text{ eV}$), the Lorentzian fit of the linewidth for the resonance mode is about $2\hbar\gamma \approx 0.0010\text{ eV}$. The Q value is 1790, being much higher than on the higher energy side. Actually, the Q factor of the microcavity depends on both the absorption coefficient and the wavelength of the light. For the excitonic luminescence of the QDs, the QDs absorb part of the emitting light, causing a damping of the light when it propagates along the internal surface of microsphere, such absorption will suppress the intensity of resonance peaks. However, because a Stokes shift exists between the intrinsic PL peak and the absorption peak, the absorption coefficient is reduced at the lower energy part of the luminescence peak, and is beneficial to reach

a higher Q factor. In fact, when the emission of QDs is employed to produce stimulated emission, i.e., lasing of the emission, in general, the active media inside of the cavity may have a nonnegligible absorption. The absorption will be an inherent issue for the cavities containing the active media. However, when there is a strong carrier injection or optical excitation which pumps and inverts the population of the carriers, the gain may become greater than the loss and then will cause lasing. Since we have found that the $\text{CdSe}_x\text{S}_{1-x}$ QDs in the microspheres have very good optical gain, especially under strong excitation conditions, the microcavity is eventually very promising for the potential lasing action, i.e., to realize the net gain at the resonance modes under relatively low excitation intensity. On the other hand, for the PL peak at lower energy side which is induced by the transitions of surface defect states, the absorption coefficient is very small in this energy region because of the limited density of states of the defects, so the intensity of resonance peaks at the lower energy side is stronger, and the Q factor is higher, which is, therefore, very suitable for the possible light storage applications and for the laser operation. From these results we can conclude that by embedding the nanocrystals in the cavity, a strong coupling between photonic and electronic states have occurred.

In summary, we have embedded the $\text{CdSe}_x\text{S}_{1-x}$ QDs in glass microspheres and observed the resonance modes with high Q factors. This way of preparing microspheres has unique advantages and is controllable. The microsphere combined with the optical fiber is expected to be utilized as a stable near-field scanning optical microscope optical probe with high sensitivity and high spatial resolutions, or it can be used for photostorage device applications.¹⁶

This work is supported by National Nature Science Foundation of China under Grant No. 29890217, and by the Project under Grant No. 69876037. The authors are grateful for the illuminating discussions of Professor U. Woggon.

¹D. Bimberg, N. Kirstaetsov, and M. Grundmann, *Phys. Status Solidi B* **75**, 3267 (1996).

²H. Sairo, K. Vishi, and I. Ogura, *Appl. Phys. Lett.* **69**, 3140 (1996).

³M. V. Maximov, Yu. M. Shernyakov, and A. F. Tsatsul'nikov, *J. Appl. Phys.* **83**, 5561 (1998).

⁴K. Mukai, Y. Nakata, and K. Otsubo, *IEEE Photonics Technol. Lett.* **11**, 1205 (1999).

⁵P. L. Huffaker and D. G. Deppe, *Appl. Phys. Lett.* **70**, 1781 (1997).

⁶R. Schur, F. Sogawa, M. Nishioka, S. Ishida, and Y. Arakawa, *Jpn. J. Appl. Phys., Part 2* **36**, L357 (1997).

⁷R. K. Chang and A. J. Chamillo, *Optical Process in Microcavities* (World Scientific, Singapore, 1996).

⁸M. V. Artemyev and U. Woggon, *Appl. Phys. Lett.* **76**, 1353 (2000).

⁹N. F. Borrelli, D. W. Hall, H. J. Holland, and D. W. Smith, *J. Appl. Phys.* **61**, 5399 (1987).

¹⁰U. Woggon, *Optical Properties of Semiconductors Quantum Dots*, Springer Tracts in Modern Physics Vol. 136 (Springer, Berlin, 1997).

¹¹D. Bersani and P. P. Lottici, *Phys. Status Solidi B* **174**, 575 (1992).

¹²D. S. Jiang, G. H. Li, H. X. Han, Y. B. Chen, and B. Q. Sun, *Chin. J. Semicond.* (in press).

¹³J. B. Xia, *Phys. Rev. B* **40**, 8500 (1989).

¹⁴K. Chang, *J. Appl. Phys.* **84**, 1454 (1998).

¹⁵P. W. Barber and R. K. Chang, *Optical Effects Associated with Small Particles* (World Scientific, Singapore, 1998).

¹⁶K. Sasaki, H. Fujiwara, and H. Masuhara, *Appl. Phys. Lett.* **70**, 2647 (1997).